Publication Year	2007
Acceptance in OA@INAF	2023-02-02T16:11:34Z
Title	A simple K-band waveguide-to-microstrip probe transition
Authors	NAVARRINI, Alessandro; PISANU, Tonino; MARIOTTI, SERGIO; Idda, Tonio
DOI	10.1002/mop.22558
Handle	http://hdl.handle.net/20.500.12386/33126
Journal	MICROWAVE AND OPTICAL TECHNOLOGY LETTERS
Number	49

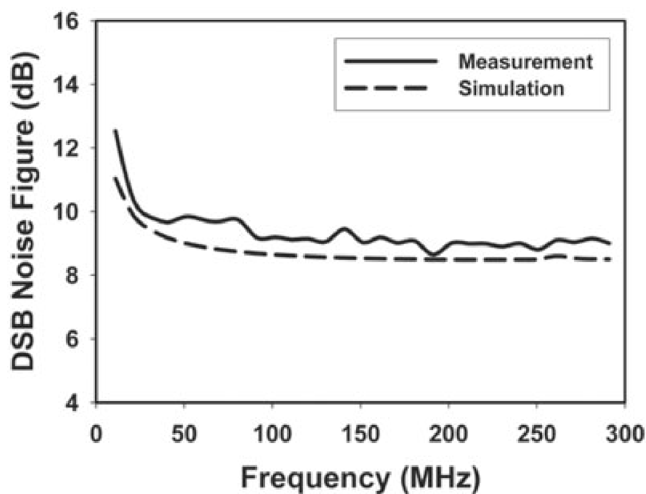

Figure 6 DSB Noise Figures of simulation and measurement for Band 1

about 1 dB higher than the simulated data, which is partly caused by added noises injected from the dc supply and an imperfect noise model of MOSFETs.

In Table 1, important parameters such as DSB NF, conversion gain, linearity, and power consumption of the proposed mixer are summarized. The proposed mixer will be useful for UWB applications of the direct conversion architecture due to the low noise and flat conversion gain for each band.

4. CONCLUSION

This article has presented a new down-conversion mixer, improved the conventional Gilbert-cell with an internal inductor and a current bleeding method. The proposed mixer topology, designed in 0.18 μm RF CMOS technology, demonstrated an excellent performance with simulation and measurement. It should be suitable for UWB systems as well as other wideband direct-conversion applications because it provides low 1/*f* noise and flat conversion gain over 3–10 GHz.

ACKNOWLEDGMENT

The authors thank H.-T. Kim of Samsung Advanced Institute of Technology for providing their 0.18 μm RF CMOS process. This research was supported by the "MIC (Ministry of Information and Communication), Korea, under the ITRC (Information Technology Research Center) support program supervised by the IITA (Institute of Information Technology Assessment)" (IITA-2006-C1090–0603-0019).

TABLE 1 Performance Summary of the Proposed Mixer

Parameters	Measure ment Results	
Technology	0.18 μm RF CMOS	
RF frequency (GHz)	3.168–10.296	
BB frequency (MHz)	264	
Bands (GHz)	Band 1 (3.168–3.696)	Band 13 (9.768–10.296)
Conversion gain (dB)	8.8 ± 1.3	0.1 ± 1.5
DSB NF (dB)	8.8–12.5	12.2–17.6
P_1dB (dBm)	−16.5	−14.2
IIP_3 (dBm)	−6.2	−4.4
Supply voltage (V)	1.8	
Power consumption (mW)	13.24	
Die size (mm^2)	0.86 × 0.86	

REFERENCES

1. http://www.ieee802.org.5/pub/TG3a.html
2. B. Razavi, RF microelectronics, Prentice Hall, Upper Saddle River, NJ, 1998.
3. B. Razavi, Design of analog CMOS integrated circuits, McGraw Hill, New York, 2001.
4. D. Manstretta, R. Castello, and F. Svelto, Low 1/*f* CMOS active mixers for direct conversion, IEEE Trans Circ Syst 48 (2001), 846–850.
5. T. Melly, A. Porret, E.A. Vittoz, and C.C. Enz, An analysis of Flicker noise rejection in low-power and low-voltage CMOS mixers, IEEE J Solid-State Circ 36 (2001), 102–109.
6. H. Darabi, and A.A. Abidi, Noise in RF CMOS mixers: A simple physical model, IEEE J Solid-State Circ 35 (2000), 15–25.
7. Q. Li and J.S. Yuan, Linearity analysis and design optimization for 0.18 μm CMOS RF mixer, IEE Proc Circ Dev Syst (2002), 112–118.
8. K. Kivekas, A. Parssien, J. Jussila, J. Ryynanen, and K. Halonen, Design of low voltage active mixer for direct conversion receivers, IEEE Int Symp Circ Syst (2001), 382–385.
9. L.A. MacEachern and T. Manku, A charge-injection method for gilbert cell biasing, IEEE Canadian Conf (1998), 365–368.
10. D. Manstretta, M. Brandolini, and F. Svelto, Second-order intermodulation mechannisms in CMOS downconverters, IEEE J Solid-State Circ 38 (2003), 394–406.
11. T.A. Phan, C.W. Kim, M.S. Kang, and S.G. Lee, Low noise and high gain CMOS down conversion mixer, IEEE Int Conf Commun Circ Syst (2004), 1191–1194.

© 2007 Wiley Periodicals, Inc.

A SIMPLE K-BAND WAVEGUIDE-TO-MICROSTRIP PROBE TRANSITION

Alessandro Navarrini,[1] Tonino Pisanu,[1] Sergio Mariotti,[2] and Tonio Idda[1]
[1] INAF, Osservatorio Astronomico di Cagliari, Loc. Poggio dei Pini, Strada 54, I-09012 Capoterra (CA), Italy
[2] INAF, Istituto di Radioastronomia, Via Gobetti 101, 40129 Bologna, Italy

Received 17 November 2006

ABSTRACT: *We describe the design, construction, and test of a simple K-band waveguide-to-microstrip transition based on a radial-shaped probe patterned on a quartz substrate. From 16 to 28 GHz, the measured reflection coefficient at the coaxial SMA input, used for test purposes of the adapter, was less than −14 dB, and the dissipative loss was ~0.30 dB. The estimated loss of the waveguide to microstrip transition only, with coaxial connector effects removed, is ~0.08 dB.* © 2007 Wiley Periodicals, Inc. Microwave Opt Technol Lett 49: 1597–1600, 2007; Published online in Wiley InterScience (www.interscience.wiley.com). DOI 10.1002/mop.22558

Key words: *waveguide adapter; radial probe; waveguide to microstrip transition; quartz substrate; low loss*

1. INTRODUCTION

Many waveguide planar probe transitions have been proposed over the years with probe orientations that were either parallel or perpendicular to the propagation direction of the waveguide [1–3]. In both cases, the probe, patterned on a dielectric substrate, enters the waveguide through a rectangular window on the broadwall of the waveguide. Probes in both configurations have been successfully designed at millimeter wavelengths to cover the full waveguide bandwidth. However, the symmetrical broadside mounted probe, where the substrate is perpendicular to the waveguide axis requires either a more complex design of the

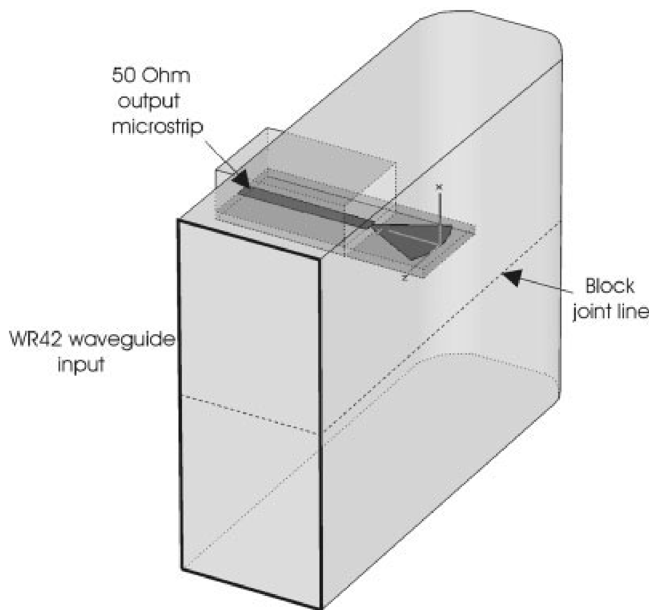

Figure 1 Internal view of the waveguide to microstrip transition with longitudinally mounted probe

mechanical blocks (for example by inserting separate waveguide short-circuit pieces at the ends of the waveguide) or employ less standard fabrication techniques for the waveguide (like the spark erosion.) Alternatively, the longitudinally mounted probe, where the substrate is parallel to the waveguide propagation axis (Fig. 1) has the advantage that the rectangular waveguide is cut along its midplane (*E*-plane) and the transition can more easily be fabricated in two block halves using a CNC milling machine.

We present the design and test results of a K-band broadband waveguide-to-microstrip transition where the same chip can be mounted either parallel or perpendicular to the waveguide axis with similar electromagnetic performance. Only the transition with longitudinally mounted probe was fabricated and tested.

2. DESIGN

Figure 1 shows an internal view of the designed waveguide to microstrip transition with longitudinally mounted probe. The two-port system consists of a radial probe on a quartz substrate that couples energy out of the waveguide. At the microstrip feed point, a quarter wave impedence transformer is used to match the probe input impedance to a on-chip 50-Ω microstrip. The probe and the substrate extend partially inside the standard WR42 waveguide (10.67 mm × 4.32 mm). The transition was optimized using electromagnetic simulation with the FDTD commercial package CST Microwave Studio (CST Microwave Studio. Büdinger Str. 2 a, D-64289 Darmstadt, Germany). Two transition configurations were studied with chip orientations either parallel or perpendicular to the waveguide axis. The parameters (probe length and opening angle, quartz width and thickness, etc.) were optimized so that the same chip would perform satisfactorily for both substrate orientations. Only the longitudinal probe configuration was retained for the final blocks fabrication and test. The double-orientation feature of the probe adds more flexibility when designing the mechanical blocks that host the transition. The simulation results for the reflection coefficient seen at the chip 50-Ω microstrip output, for chip orientation either parallel or perpendicular to the waveguide axis, are shown in Figure 2: the reflection coefficient is below −20 dB across 18–26.5 GHz. For the chip, we used the following

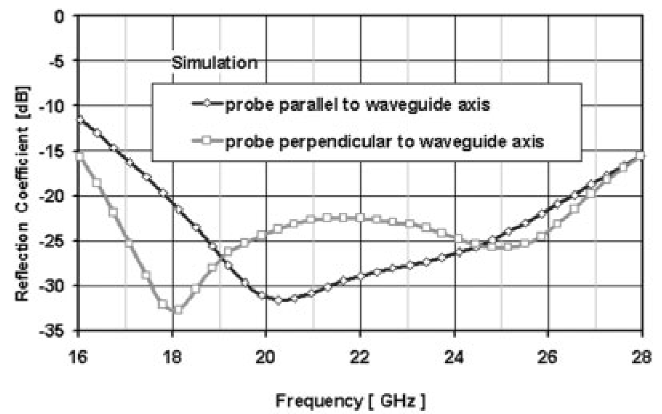

Figure 2 Simulated reflection coefficient at the 50- Ù microstip chip port for probe orientation parallel (longitudinal probe, rhomb dotted line) and perpendicular (broadside probe, square dotted line) to the waveguide axis

parameters: probe radius 2.28 mm, probe opening angle 60°, quartz substrate width 2.79 mm, thickness 0.25 mm, air gap above 1.27 mm, interconnecting microstrip line width 0.46 mm, length 1.98 mm, output microstrip line width 0.51 mm, length 0.44 mm. The fixed backshort is located at 3.81 mm from the chip symmetry axis in the longitudinal configuration, and at 4.32 mm from the probe (with metallization looking away from the backshort) in the broadwall configuration ($\sim\lambda_g/4$).

3. FABRICATION

The chip, shown in Figure 3, has dimensions 0.25 mm × 2.79 mm × 6.50 mm. It was fabricated by Diablo Industries (Diablo Industries, 2254 Meridian Boulevard, Suite E, Minden, NV 89423, http://www.ditf.com). The top side of the chip is patterned with the metallized radial probe and microstrips, while the ground plane on the backside of the substrate is partially truncated to cover the microstrip sections only. On both chip sides, the thin film metallization consists of two layers, with a 3.5-μm-thick gold on top of 0.25 μm titanium-tungsten alloy (Ti/W) adhesive layer used to

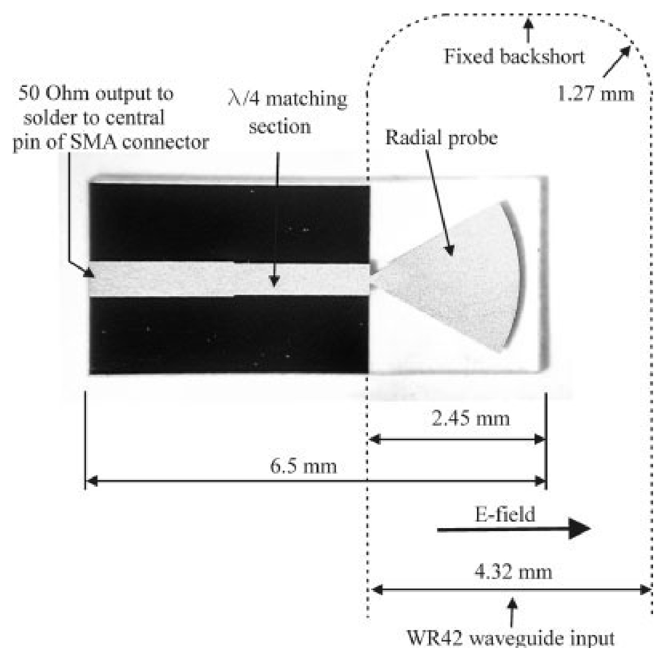

Figure 3 Photo of the chip in longitudinally mounted configuration

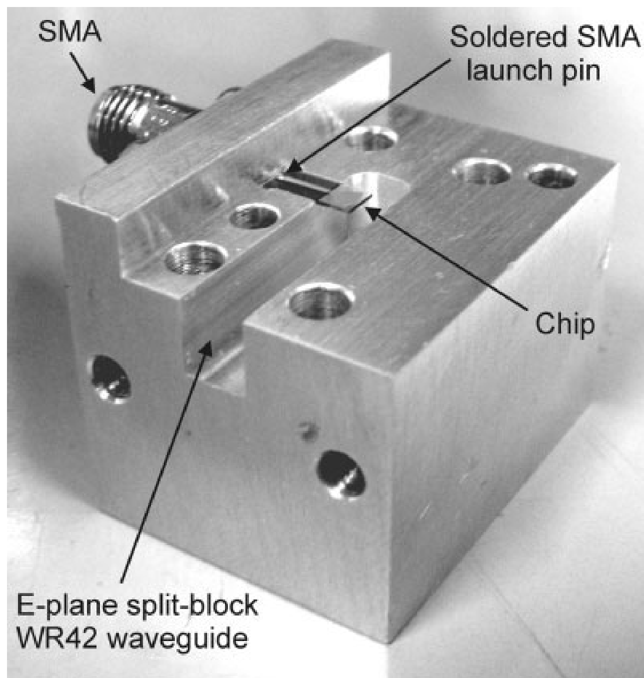

Figure 4 Photo of one of the two mating blocks with embedded chip. The input rectangular waveguide is cut along the *E*-plane. The external dimensions of the two assembled blocks (excluding the SMA connector) are 23.3 × 29.5 × 40.0 mm^3

glue the gold on the quartz substrate. The gold thickness was chosen to be several times the skin depth at the frequency of interest (δ_{Au} (22 GHz) ~0.5 μm). The room temperature bulk electrical conductivity of the alloy (10% Ti and 90% W) is 1.05 × 10^6 S/m, 40 times worst than gold (42.5 MS/m) (applications of high conductivity traces in thin film circuits, Aeroflex—MIC Technology Corporation, 1995). To evaluate the contribution to the ohmic loss due to the additional Ti/W layer, we performed simulations with TRL.EXE (TRL.EXE Compact Software (now Ansoft Corporation)) of the 0.51 mm wide 50-Ω microstrip at the chip output, with and without the Ti/W layer. At the central frequency, 22 GHz, the simulated room temperature, conductor loss per unit length of the single-layer pure gold microstrip is 0.099 dB/cm; only 3% less than the two-layer one, which is 0.102 dB/cm. The total loss of the two-layer microstrip is 0.108 dB/cm, of which 0.06 dB/cm are due to dielectric loss. These simulations indicate that the very thin Ti/W layer contribute only slightly to the total microstrip loss.

A coaxial SMA connector (Southwest Microwave Super SMA model SWMI 214–538SF with 1490–11G launch pin and dielectric for 4.75-mm-thick metal wall) was connected to the chip 50-Ω microstrip output for test purposes. The adapter was fabricated using two aluminium alloy pieces with blocks joint line located along the *E*-plane of the waveguide. Dowel pins (3 mm diameter) were used to align the blocks. One of the two mating blocks is shown in Figure 4. The block includes the channel to house the chip and the SMA connector. We aligned the border line defined by the partially metallized ground plane and the uncovered part of the chip at the substrate bottom, with the prolongation of the waveguide walls, i.e. the channel end. We used silver loaded epoxy (Epotek H20E, Epoxy Technology, 14 Fortune Drive, Billerica, MA 01821-3972) to glue the chip ground plane on the aluminium block channel. To connect the chip microstrip output to the central launch pin of the SMA connector, we first used the same Epoxy, later we replaced it with SnPb solder alloy. Neither cases showed metallurgical incompatibility between silver epoxy and aluminium alloy or SnPb alloy and gold.

The simulated loss of the waveguide to microstrip transition only, with SMA and solder effects removed, was ~0.08 dB.

4. MEASUREMENTS

Two identical adapters were fabricated, assembled, and tested both individually and back-to-back using an HP 8722D vector network analyzer (VNA). The estimated, worst case measurement uncertainty is ±0.06 dB for the typical values of transmission and ±0.5 dB for the typical values of reflection.

We calibrated the VNA using two different methods: the adapter removal method (including the sliding termination) to test the adapters individually, and the TRL method to test the adapters back-to-back. Care was taken to minimize the drift by reducing the cables movement and by keeping the room temperature very stable.

The two sets of different measurements performed with the two different calibration methods on individual adapters gave very similar results. Also, the two adapters have very similar performances. Figure 5 shows the available gain between the SMA port and the waveguide port of one of the adapters. Since the adapter will be placed in front of a low-noise amplifier, it is important to estimate its contribution to the noise temperature. The available gain (G_{av}) is the figure of merit in noise temperature budget calculations. For linear, reciprocal, low-loss devices driven by a reflectionless source, it is possible to write $G_{av} = -$dissipative loss (later, simply "loss") [4]. The available gain varies in the range −0.75 to −0.48 dB (round dot line) across 16–28 GHz. We found that, soldering the SMA central pin to the chip with SnPb alloy (Stannol GmbH, 0.5 mm dia solder wire Sn62Pb36Ag2), rather than with silver loaded epoxy, improved the average loss of about 0.22 dB across the band: the available gain of the adaptor with SnPb was in the range −0.45 to −0.26 dB (square dot line). Care was taken to remove the epoxy and replace it with SnPb to make sure neither to move the chips nor the connectors inside the blocks so that the change in measured insertion loss would only reflect the change in solder type. We repeated the two sets of measurements when using the two different solders on the second adapter and

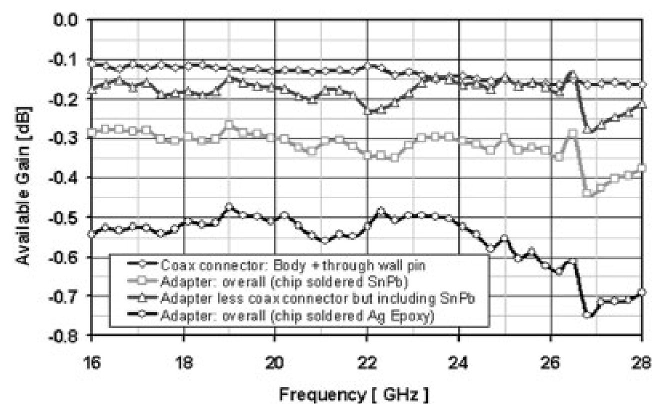

Figure 5 Available gain of one of the two adapters: the lower round dotted and square dotted lines at the bottom are, respectively, the measured gain when epoxy and SnPb were used to solder the central pin of the SMA to the chip output. The top rhomb dotted line is the measured gain of a single SMA connector and trough wall pin. The triangle dotted line is the estimated gain of the chip embedded in the waveguide structure, with SMA effects removed

TABLE 1 22 GHz Loss Budget

WR42 Waveguide Section	Chip	Soldering	SMA Connector	Adapter Total
From Literature 0.02 dB	From Simulation 0.06 dB	From Difference 0.14 dB (SnPb) 0.33 dB (Ag epoxy)	From Measurement and Simulation 0.12 dB	From Measurement 0.34 dB (SnPb) 0.53 dB (Ag epoxy)

obtained very similar results that confirmed the 0.22 dB higher transmission of the transition soldered with SnPb.

To evaluate the contribution of the SMA transition to the total loss of the adapter, we measured two SMAs back-to-back, halved this value, and added ~0.06 dB, which is the simulated loss accounting for the 4.75 mm long 50-Ω coaxial line of the SMA launch pin (diameter 0.23 mm) and dielectric tab (external diameter 0.74 mm) inserted into the aluminium block of the adapter.

An aluminium WR42 waveguide has theoretical loss in the range 0.42–0.59 dB/m [5]. Therefore, for our 19-mm long waveguide section of the adapter, the estimated loss, corrected for the finite surface roughness of the material, are of the order of ~0.02 dB. Considering that the predicted loss of the chip is ~0.06 dB, we derive that, in order to explain the measured loss of a single adapter where chip and SMA are soldered with SnPb, the loss due to the solder should account for ~0.14 dB (the room temperature electrical conductivity of the SnPb is 6.9 MS/m, about 16% of the gold bulk conductivity).

The triangle dotted line in Figure 5 shows the estimated available gain, of ~−0.2 dB, of the waveguide-to-microstrip transition soldered with SnPb, where the SMA effects were removed. Similarly, we estimate that the contribution to the loss due to the epoxy solder that connects the chip to the SMA accounts for ~0.33 dB (the room temperature electrical conductivity of the epoxy is specified to be bigger than 0.25 MS/m, which could be as low as 0.59% of the gold conductivity). A summary of the loss budget at 22 GHz is shown in Table 1.

Figure 6 shows the reflection coefficient measured at the SMA port of a single adaptor soldered with SnPb and epoxy. The reflection coefficient is below −14 dB across 16–28 GHz in both cases. The measured reflection is higher than predicted by simulation.

5. CONCLUSIONS

We designed a broadband waveguide-to-microstrip transition based on a radial-shaped probe patterned on a quartz substrate. The chip can be mounted with orientations either parallel or perpendicular to the propagation direction of the waveguide with similar performance. Only the transition in longitudinal configuration was fabricated and tested. An SMA connector was connected at the chip output for test purposes using first silver epoxy, then SnPb alloy. From 16 to 28 GHz, the measured reflection coefficient on both directions was less than −14 dB and the loss was ~0.3 dB when SnPb was used. The estimated loss of the waveguide to microstrip transition only, with SMA and solder effects removed, was ~0.08 dB. Use of SnPb alloy solder instead of epoxy decreased the average loss of 0.22 dB across the band.

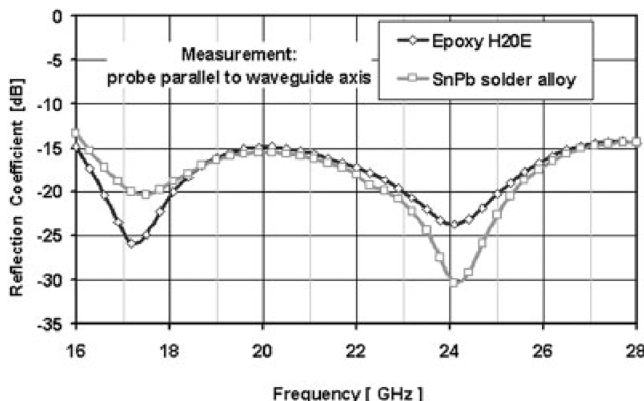

Figure 6 Reflection coefficient measured at the SMA input of one of the adaptors (with its output terminated in a waveguide load) soldered with SnPb and epoxy

REFERENCES

1. Y.-C. Leong and S. Weinreb, Full-band waveguide to microstrip probe transition, IEEE microwave theory and techniques, digest of papers, Anaheim, CA, June 13–19, 1999.
2. Y.-C. Shih, T.-N. Ton, and L.Q. Bui, Waveguide-to-microstrip transitions for millimetre-wave applications, IEEE MTT-S Int Microwave Symp Dig, New York, NY, (1988) 473–475.
3. A. Navarrini, D. Billon-Pierron, K.F. Schuster, and B. Lazareff, Design of a 275–370 GHz SIS mixer with image sideband rejection and stable operation, Proceedings of the 12th International Symposium on Space Terahertz Technology, San Diego, California, USA, February 14–16, 2001, pp. 205–214.
4. F.L. Warner Microwave attenuation measurement, IEE Press, IEE monograph series, 19, 1977, p. 8.
5. Flann Microwave Products Catalog 2006, p. 122.

© 2007 Wiley Periodicals, Inc.

A NEW WIDEBAND THREE-WAY POWER DIVIDER

Guan-Yu Chen and Jwo-Shiun Sun
Department of Electronic Engineering, National Taipei University of Technology, Taiwan

Received 23 November 2006

ABSTRACT: *A new three-way power divider that provides equal power split over a wide bandwidth implemented on a single-layer printed circuit board (PCB) is presented. It can be easily extended to an arbitrary number of output ports. The proposed power divider exhibits fairly good performance validated by measurement and simulation. Measured results show that the three output ports across the bandwidth from 1.8 to 10.5 GHz for 10 dB return loss are attainable.* © 2007 Wiley Periodicals, Inc. Microwave Opt Technol Lett 49: 1600–1603, 2007; Published online in Wiley InterScience (www.interscience.wiley.com). DOI 10.1002/mop.22547

Key words: *power divider; microstrip; wideband*

1. INTRODUCTION

Power dividers provide simple, repeatable performance improvements for antenna array systems and are widely used in microwave, communication, and high frequency operations. The Wilkinson power divider was invented in 1960 [1] with good output